

Dichromatic Based Rendering of Texture Images with High Color Fidelity

H. L. Shen and J. H. Xin

Institute of Textiles & Clothing, The Hong Kong Polytechnic University, Hong Kong

In this study, an algorithm was developed for the rendering of texture images with high color fidelity. The algorithm is based on the dichromatic reflection model, which recovers the implicit geometrical information of each pixel position in the texture image by exploiting the interaction between object surface and light. Using the recovered implicit geometrical information and a target color, a new texture image can then be synthesized. The synthesized image was then further modified to give correct texture strength. The algorithm developed in this study can be used for both color and gray texture images. It is suitable for the applications in texture simulation and visualization with the advantage of high color fidelity.

Journal of Imaging Science and Technology 48: 246–250 (2004)

Introduction

The perception of color and texture is the result of a complicated interaction between illumination and geometry variation of the object surfaces. Recently, texture synthesis has been extensively studied in the literature of computer graphics and computer vision,^{1–3} in attempt to simulate new and realistic texture images from samples. However, there are still limited works dealing with the color fidelity in texture synthesis.^{4,5} Xin and Shen⁴ investigated the proportionality of the pixel deviation to the mean color in each channel and proposed a computational model for the color mapping on texture images. Their method performed well on regular and homogeneous texture images, but the assumption of the proportionality may fail for textures with high contrast. In the study of the texture effect on suprathreshold lightness tolerances, Montag and Berns presented a method of texture image simulation.⁵ They first produced a decorrelated color space (DCS) using singular value decomposition (SVD), then modified the mean color of the image, and finally inverted the color transform to generate new texture images. It was noticed that the DCS produced using singular value decomposition is image related, which means that the optimal DCS for the original image may not be the optimal for the reproduced images with other colors. In fact, the spatial color distribution of texture images is attributed to the geometrical structure of the texture samples. Although the previous

methods^{4,5} performed well in texture and color simulation, they could not describe all the pixels accurately, as they are based on the statistical information and do not consider the geometrical factors.

In this study, we attempted to synthesize color texture images from a given image with high color fidelity based on the fundamental interaction between light and the object surfaces. The geometrical information of the texture surface is firstly recovered based on the dichromatic reflection model.⁶ This was then followed by the synthesis of new color texture images from the recovered geometry and target solid colors. The texture strength of the synthesized images was further modified according to the target colors. As the dichromatic reflection model is physics-based and holds well for the description of a large variety of materials,^{7,8} the high fidelity of the synthesized texture images can therefore be reliably achieved. The characterization of the imaging device (color scanner) was performed by recovering its spectral responsivity. This spectral responsivity can also enable the direct use of the spectral reflectance values as a new target color for rendering. The algorithm proposed in this article can be applied to both gray and color texture images, and is applicable in the applications of texture simulation and visualization.

In traditional fabric design process, for example, the color appearance of the designs using different colored yarns can only be visualized through the processes of coloration, weaving, or knitting, which are very time consuming. As the final fabric designs are textured, there are demands to render solid color onto various different texture patterns for the visualization of the appearance of final products. Considering the importance of color quality in the textile and apparel industries, the proposed algorithm emphasizes the rendering of texture images that can achieve perceptual similarity to the actual materials with a high degree of color fidelity. In addition, the proposed algorithm provides an alternative texture simulation method for investigating the relationship between texture patterns and tolerance threshold of color difference.⁵

Original manuscript received July 1, 2003

Supplemental Material—Figures 4 and 5 can be found in color on the IS&T website (www.imaging.org) for a period of no less than two years from the date of publication.

txinjh@inet.polyu.edu.hk; tel: +852 2766 6474; fax: +852 2773 1432

©2004, IS&T—The Society for Imaging Science and Technology

Algorithm of Color Rendering of Texture Images

The output of a typical color imaging device, such as color scanner, is a three-band image with red, green, and blue channels. For simplicity, it is assumed that illumination is spatially uniform and the indices expressing spatial coordinates are omitted. Provided that the imaging system is linear, the response at pixel position i by the k th sensor is given by

$$V_k^i = \int L(\lambda) S_k(\lambda) R(i; \lambda) d\lambda \quad k = 1 \dots 3 \quad (1)$$

where $L(\lambda)$ is the light illumination, $S_k(\lambda)$ is the spectral sensitivity function of the k th sensor, and $R(i; \lambda)$ is the reflectance at position i .

According to the dichromatic reflection model,⁶ the reflected light can be decomposed into two components namely a surface reflection and a body reflection. The surface reflection occurs at the object surface, and its spectral composition is approximately the same as that of the illumination. The body reflection is the result of the scattering of the light within the pigmented layer of the object subsurface and the selective absorption of the light dependent on the material characteristic. It is further assumed in the dichromatic reflection model that the surface and the body reflection can be further decomposed into two independent components, i.e., spectral and geometric ones. Therefore, the reflectance $R(i; \lambda)$ can be written as

$$R(i; \lambda) \approx m_b(i) R_b(\lambda) + m_s(i) R_s(\lambda) \quad (2)$$

where $m_b(i)$ and $m_s(i)$ are the geometric factor of the body and the surface reflection at position i , and $R_b(\lambda)$ and $R_s(\lambda)$ are the wavelength composition of the body and the surface reflectance respectively. As the spectral composition of the surface reflection is the same as that of the illumination, $R_s(\lambda)$ is a constant R_s and Eq. (2) becomes

$$R(i; \lambda) \approx m_b(i) R_b(\lambda) + m_s(i) R_s \quad (3)$$

Substituting Eq. (3) into Eq. (1) yields

$$V_k^i = m_b(i) V_b^k + m_s(i) V_s^k \quad (4)$$

where

$$V_b^k = \int L(\lambda) S_k(\lambda) R_b(\lambda) d\lambda, \text{ and } V_s^k = R_s \int L(\lambda) S_k(\lambda) d\lambda \quad (5)$$

Equation (4) can be written in the vector form as

$$\mathbf{V}^i = m_b(i) \mathbf{V}_b + m_s(i) \mathbf{V}_s \quad (6)$$

where \mathbf{V}^i is the 3×1 color vector at pixel i , \mathbf{V}_b and \mathbf{V}_s is the 3×1 vector of body color V_b^k and surface color V_s^k , respectively. The body color \mathbf{V}_b is closely related to the characteristic of the material, and \mathbf{V}_s is determined by the given imaging system and the illumination condition. Let N be the pixel number of the texture image, the mean color of the image can be calculated as

$$\begin{aligned} \bar{\mathbf{V}} &= \frac{1}{N} \sum_{i=1}^N \mathbf{V}^i \\ &= \frac{1}{N} \sum_{i=1}^N m_b(i) \mathbf{V}_b + \frac{1}{N} \sum_{i=1}^N m_s(i) \mathbf{V}_s \\ &= \bar{m}_b \mathbf{V}_b + \bar{m}_s \mathbf{V}_s \end{aligned} \quad (7)$$

where \bar{m}_b , \bar{m}_s is the mean geometrical term of the body and surface reflection, respectively. As both of \mathbf{V}^i and $\bar{\mathbf{V}}$ are the linear combination of \mathbf{V}_b and \mathbf{V}_s , equation 6 and 7 can be combined by deleting the term body color \mathbf{V}_b

$$\mathbf{V}^i = \alpha_i \bar{\mathbf{V}} + \beta_i \mathbf{V}_s \quad (8)$$

where

$$\alpha_i = \frac{m_b(i)}{\bar{m}_b} \text{ and } \beta_i = \frac{m_s(i) \bar{m}_b - m_b(i) \bar{m}_s}{\bar{m}_b} \quad (9)$$

Accordingly (α_i, β_i) is the geometrical coefficient pair that completely defines the relative geometry of the pixel i with respect to that of the mean color.

In the case that the original texture image is a color one, the color vector $\bar{\mathbf{V}}$ and \mathbf{V}_s are generally not of the same direction, i.e.,

$$\frac{\bar{\mathbf{V}} \cdot \mathbf{V}_s}{\|\bar{\mathbf{V}}\| \cdot \|\mathbf{V}_s\|} \neq 1. \quad (10)$$

As Eq. (8) is over-determined (three channels and two unknowns), the coefficient pair (α_i, β_i) can be solved using the least squares method. Also, the coefficient pair (α_i, β_i) holds the properties that

$$\frac{1}{N} \sum_{i=1}^N \alpha_i \approx 1 \text{ and } \frac{1}{N} \sum_{i=1}^N \beta_i \approx 0 \quad (11)$$

The color \mathbf{V}_s is actually the white point of the imaging system. It can be directly measured using an ideal white diffuser. If the white point is not available, \mathbf{V}_s can be approximately assumed to be $\mathbf{V}_s = [1 \ 1 \ 1]^T$, where the superscript T denotes vector transpose. In this case, the algorithm is called the color-color (C-C) method.

In the case that the original texture image is a grayscale one (that is, $k = 1$), the geometrical coefficient pair (α_i, β_i) can be easily solved as

$$\alpha_i = \frac{V_k^i}{V_k}, \quad \beta_i = 0. \quad (12)$$

Accordingly, the algorithm is called the gray-to-color (G-C) method in this case.

After the geometrical coefficient pair (α_i, β_i) is calculated in either the C-C method or the G-C method, the color of the pixel i can be synthesized from a target solid color $\bar{\mathbf{U}}$ as

$$\mathbf{U}^i = \alpha_i \bar{\mathbf{U}} + \beta_i \mathbf{V}_s \quad (13)$$

where \mathbf{U}^i and $\bar{\mathbf{U}}$ are the color vectors of element U_k^i and \bar{U}_k , respectively.

It is known that the texture strength for each color channel is correlated to the lightness of the color. To simulate this characteristic of the texture images, the texture strength should be further modified according to the target color. In this study, the texture strength was approximately represented by the standard deviation σ_k of a texture image. For single-colored regular images with similar texture pattern, σ_k can be approximately derived from the mean color \bar{V}_k . Figure 1 shows a typical relationship between the standard deviation and mean color for texture images of knitted textile fab-

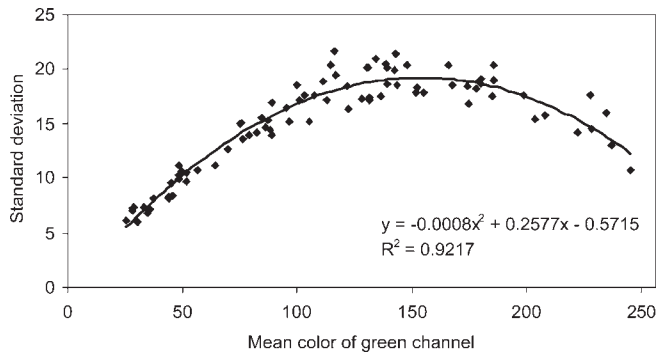


Figure 1. Typical relationship between standard deviations and mean colors.

rics, where the relationship can be fitted by a 2nd-order polynomial equation with a high correlation coefficient.

After the establishment of the relationship between the standard deviation and the mean color, the pixel color of the k th channel can be modified as

$$U_k^i = \bar{U}_k + \frac{\sigma_k'}{\sigma_k} (U_k^i - \bar{U}_k) \quad (14)$$

where σ_k and σ_k' are the standard deviation of the k th channel of the synthesized image before and after texture strength modification, respectively. It should be noted that σ_k is calculated from the image \mathbf{U}^i , and σ_k' is obtained from the 2-order polynomial fitting function.

Characterization of the Imaging System

As mentioned above, the proposed algorithm of color rendering assumes the linearity of the imaging device. However, the channel outputs of imaging systems, such as digital cameras and desktop scanners, are normally nonlinear⁹⁻¹¹ as shown in Eq. (15):

$$\rho_k = F_k(V_k) = F_k\left(\int L(\lambda)S_k(\lambda)R(\lambda)d\lambda\right) \quad (15)$$

where F_k is the nonlinear function that transforms the linear response V_k to its corresponding actual nonlinear response ρ_k . The pixel position is omitted in Eq. (15) as the geometrical variation of the color patches for linearization is negligible. In this study, the texture images were obtained by scanning textile fabrics with different colors using an Epson flatbed scanner model GT-10000+.

TABLE I. Comparison of the actual linear responses V_k and predicted ones \hat{V}_k using mathematically recovered spectral responsivity. The error of a color is calculated using $|V_k - \hat{V}_k|/V_{k,max} \times 100\%$, where $V_{k,max}$ is the maximum linear response of the k th channel of the white patch of ColorChecker.

	ColorChecker			Textile fabrics		
	Red	Green	Blue	Red	Green	Blue
Mean error (%)	0.826	0.910	1.211	0.690	0.762	1.239
Maximum error (%)	2.128	3.090	4.638	3.053	3.181	4.747

To examine the nonlinearity of the scanner, the Kodak Gray Scale was scanned and the average RGB values for the twenty gray patches were calculated in a centered 40×80 window. The spectral reflectance of each gray patch was measured using the GretagMacbeth Color-Eye 7000A spectrophotometer. The reverse nonlinear function F_k^{-1} is therefore can be regarded as the monotonically increasing nonlinear curve between the actual response of the scanner and the average reflectance ($\times 100$) of the gray patches. It was found that the F_k^{-1} of the red, green and blue channels were very similar to one another. In the application, the F_k^{-1} served as a lookup table and the linear response of the scanner were calculated by linear interpolation and extrapolation.

In order to obtain the spectral responsivity, some constraints such as smooth and positivity should be added, and the solution can be viewed as a quadratic programming problem or a constrained linear least squares method.¹⁰ In this study, the twenty-four color patches on the GretagMacbeth ColorChecker were used for the calculation of the spectral responsivity. In order to check its accuracy and general, twenty-four textile fabrics with distinct colors were used for testing. The comparison between the actual and predicted linear responses for these two target sets are given in Table I. The prediction errors of the linear response of the ColorChecker were very low. The error of the blue channel was slightly higher than that of the red and green channels. The prediction errors of the textile fabrics were also low, which indicated that the calculated spectral responsivity was also applicable for this color target.

Figure 2 illustrates the scheme of the color rendering process after the linearization and characterization of the scanner. The target color for synthesis can either be in RGB format or reflectance format after scanner characterization. All the actual responses of the original texture image or the target color were transformed into their linear counterparts to be used in the algorithm as

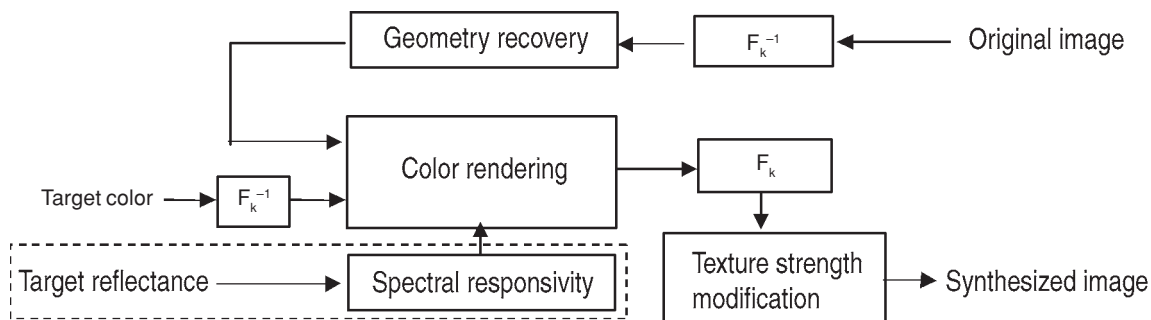


Figure 2. Schematic of the color rendering process after imaging device characterization.

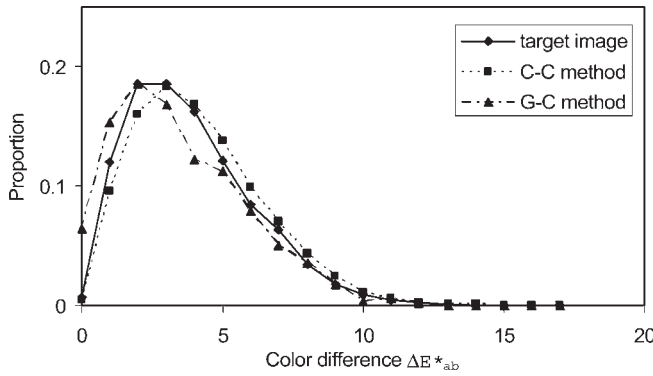


Figure 3. An example of the histograms of color difference (between the each pixel and the mean) for the target image and the synthesized images using C-C and G-C methods.

the geometry recovery and color rendering needed to be conducted in the linear color space. After the color rendering, the linear response was then reversed into the nonlinear scanner response with function F_k , and the texture strength modification was further applied to produce a color texture image.

Results and Discussion

In the experiment, given a digital image I_A of textile fabric A , we computed a simulated digital image I_B of a target textile fabric B . The mean color \bar{c}_B of the target sample B was used as the target color. We assumed that \bar{c}_B was different to the mean color \bar{c}_A of sample A . From the digital image I_A , and the colors \bar{c}_A and \bar{c}_B , we were able to simulate an image which is perceptually close to the target scanned image I_B .

The textile fabrics of both knitted and woven structures with different colors were scanned at an appropriate image resolution. In the experiment, the texture patterns of the original images and target images are approximately the same, as the purpose is to evaluate similarity of the color and texture appearance between the synthesized images and the target ones. The coefficient pair (α_i, β_i) was calculated from the original images and the mean colors of the target images were used for color rendering. The performance of the algorithm can be evaluated by comparing the synthesized texture image with the target one. As there is no pixel correspondence for the synthesized images and the target texture images, the evaluation is conducted using a statistical approach.

For each pixel in a texture image, its color difference to the mean color is calculated in the display color space. The histogram of the color difference is then constructed. An example of the histograms is shown in Fig. 3. The statistical distributions of the color difference of two synthesized images using C-C and G-C method are both similar to that of the target image. The histogram of synthesized image using C-C method is closer to the histogram of the target image than that using G-C method. This is expected as the information in C-C method is three dimensional whereas in G-C method is only one dimensional. Accordingly, the recovered geometrical pair (α_i, β_i) is accurate for the former.

Let I be the target texture image, I' be the synthesized image, and $H_j(\cdot)$ be the proportion of the j th bin of the histogram, then the image similarity can be calculated by the method of histogram intersection¹²:

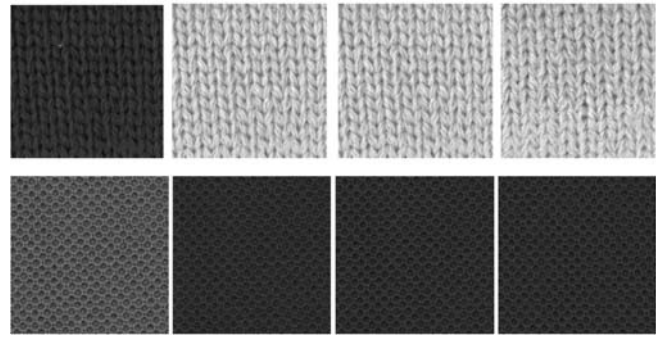


Figure 4. Synthesis results for the texture images of knitted fabric (top row) and woven fabric (bottom row). Left to right: original images; synthesized images using C-C method; synthesized images using G-C method; target images. *Supplemental Material—Figure 4 can be found in color on the IS&T website (www.imaging.org) for a period of no less than two years from the date of publication.*

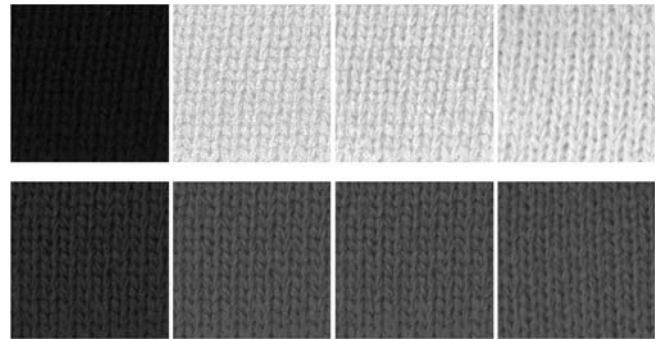


Figure 5. Synthesis results for the texture images with very dissimilar lightness (top row) and dissimilar colors (bottom row) of knitted fabric. Left to right: original images; synthesized images using C-C method; synthesized images using G-C method; target images. *Supplemental Material—Figure 5 can be found in color on the IS&T website (www.imaging.org) for a period of no less than two years from the date of publication.*

$$p(I, I') = \frac{\sum_{j=1}^N \min(H_j(I), H_j(I'))}{\sum_{j=1}^N H_j(I)} \quad (16)$$

When the texture distribution of the two image, I and I' , are quite similar, the term $p(I, I')$ should be appropriate for the assessment of the image similarity in terms of color fidelity. The more similar the target image is to the synthesized image, the closer the term $p(I, I')$ is to 1.

Examples of the synthesized results of knitted and woven fabric images using the C-C method and the G-C method are given in Fig. 4. Two other examples are presented in Fig. 5 to show the rendering effect of texture images with very dissimilar lightness and colors. The gray textures in the G-C method were obtained simply by averaging the three RGB color channels of the original images. We found that the synthesis results degrade when the lightness or colors of the original and target images are very dissimilar. For these texture images, the geometrical coefficient pair (α_i, β_i) may not be accurate enough for color synthesis. In Fig. 5, the synthesis results using G-C method are slightly better than those

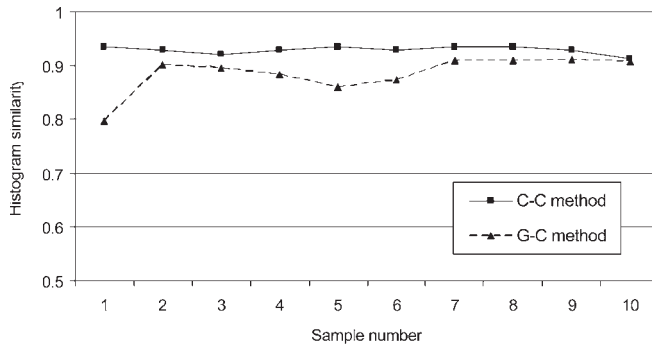


Figure 6. The image similarity between the synthesized images and the target images.

using C-C method, which may be attributed to the slight reduction of the noise when using average channel response in the G-C method. These unsatisfactory synthesis results for the texture images seems unavoidable for any method based on data from a real device like a scanner, as the signal-to-noise ratios of some channels are very low for extremely dark and vivid color images. The quantization levels are inadequate for channel responses at the low end, as indicated by the relationship between standard deviations and channel responses in Fig. 1. This was also noticed by Montag and Berns, and they simulated new texture images from original ones with similar lightness to avoid this limitation.⁵ The image similarity measurements using histogram intersection between the synthesized images and the corresponding target images are provided in Fig. 6. Both of the C-C and G-C methods produced satisfactory synthesis results. The C-C method performs slightly better than the G-C method for the great majority of texture images except the ones with extremely dark and vivid colors. Visual examination of the color appearance of the synthesized and the target texture images also indicated that they were perceptually identical.

Conclusions

An algorithm of color texture rendering with emphasis on high color fidelity has been presented. The algorithm consists of three main steps. Firstly, the necessary geometrical information of each pixel is recovered by dichromatic reflection model. Secondly, new texture images are synthesized by combining the geometrical information and target solid colors. Finally, the texture strength of the synthesized images is modified to provide high simi-

larity in color and texture perception. The synthesis algorithm can be applied on either gray or color texture images. This algorithm also takes advantages of the scanner characterization and new texture images can also be synthesized from reflectance. The experimental results verified the effectiveness of the algorithm in terms of image similarity. We note that, although only the knitted and woven textile fabrics are used as examples in this study, it does not imply the proposed algorithm can only be applicable to those materials. In fact, the dichromatic reflection model can also describe other materials including plastic and wood. However, applying the proposed color rendering algorithm to other materials is beyond the scope of this paper. A limitation of the proposed algorithm is that the synthesis results may degrade when the colors of the original and target images are very dissimilar, which is attributed to the limitation of the real imaging devices. ▲

Acknowledgment. The authors would like to acknowledge the financial support of this project from the Hong Kong Polytechnic University and the Research Grants Council of Hong Kong SAR Government (project reference: PolyU 5153/01E).

References

1. D. Heeger and J. Bergen, Pyramid-based Texture Analysis/Synthesis, *Proc. SIGGRAPH*, 229 (1995).
2. L. Y. Wei and M. Levoy, Fast texture synthesis using tree-structured vector quantization. *Proc. SIGGRAPH*, 479 (2000).
3. P. Campisi and G. Scarano, A multiresolution approach for texture synthesis using the circular harmonic functions, *IEEE Trans. Image Proc.* **11**, 37 (2002)
4. J. H. Xin and H. L. Shen, Computational model for color mapping on texture image, *J. Electr. Imaging* **12**, 697 (2003).
5. E. D. Montag and R. S. Berns, Lightness dependencies and the effect of texture on suprathreshold lightness tolerances, *Color Res. Appl.* **25**, 241 (2000).
6. S. A. Shafer, Using color to separate reflection components, *Color Res. Appl.* **10**, 210 (1985).
7. H. C. Lee, E. J. Breneman and C. P. Schulte, Modeling light reflection for computer vision, *IEEE Trans. Pattern Analysis Machine Intell.* **12**, 402 (1990).
8. S. Tominaga, Dichromatic reflection model for a variety of materials, *Color Res. Appl.* **19**, 277 (1994).
9. G. W. Hong, M. R. Lou and P. A. Rhodes, A study of digital camera colorimetric characterization based on polynomial modeling, *Color Res. Appl.* **26**, 76 (2001).
10. K. Barnard and B. Funt, Camera characterization for color research, *Color Res. Appl.* **27**, 152 (2002).
11. P. L. Vora, J. E. Farrell, J. D. Tietz, and D. H. Brainard, Image capture: modeling and calibration of sensor responses and their synthesis from multispectral images, Technique report [Internet], Hewlett-Packard Laboratory, Contract No: HPL-98-187, Available from <http://www.hpl.hp.com/techreports/98/HPL-98-187.html>.
12. M. J. Swain and D. H. Ballard, Color indexing, *Intl. J. Computer Vision* **7**, 11 (1991).